Fourier Transform Infrared Double-Flash Experiments Resolve Bacteriorhodopsin's M_1 to M_2 Transition

B. Hessling, J. Herbst, R. Rammelsberg, and K. Gerwert
Lehrstuhl für Biophysik, Fakultät Biologie, Ruhr Universität Bochum, 44780 Bochum, Germany

ABSTRACT The orientation of the central proton-binding site, the protonated Schiff base, away from the proton release side to the proton uptake side is crucial for the directionality of the proton pump bacteriorhodopsin. It has been proposed that this movement, called the reprotonation switch, takes place in the M_1 to M_2 transition. To resolve the molecular events in this M_1 to M_2 transition, we performed double-flash experiments. In these experiments a first pulse initiates the photocycle and a second pulse selectively drives bR molecules in the M intermediate back into the BR ground state. For short delay times between initiating and resetting pulses, most of the M molecules being reset are in the M_1 intermediate, and for longer delay times most of the reset M molecules are in the M_2 intermediate. The BR-M_1 and BR-M_2 difference spectra are monitored with nanosecond step-scan Fourier transform infrared spectroscopy. Because the Schiff base reprotonation rate is $k_{M1} = 0.8 \times 10^7\ s^{-1}$ in the light-induced M_1 back-reaction and $k_{M2} = 0.36 \times 10^7\ s^{-1}$ in the M_2 back-reaction, the two different M intermediates represent two different proton accessibility configurations of the Schiff base. The results show only a minute movement of one or two peptide bonds in the M_1 to M_2 transition that changes the interaction of the Schiff base with Y185. This backbone movement is distinct from the larger one in the subsequent M to N transition. No evidence of a chromophore isomerization is seen in the M_1 to M_2 transition. Furthermore, the results show time-resolved reprotonation of the Schiff base from D85 in the M photo-back-reaction, instead of from D96, as in the conventional cycle.

INTRODUCTION

Bacteriorhodopsin (bR) is a light-driven proton pump in the purple membrane of *Halobacterium salinarium* (Oesterhelt and Stoeckenius, 1971; for a recent overview, see the special issue of *Biophys. Chem.*, Retinal Proteins, 56:1–2, 1995). The primary event in the photocycle is an all-*trans*→13-*cis* isomerization of the chromophore retinal in the $BR_{570} \rightarrow J_{600}$ transition. The succeeding thermal reactions, through spectroscopically distinct intermediates K_{590}, L_{550}, M_{410}, N_{530}, and O_{640}, translocate a proton across the membrane, and the protein returns to the initial state BR_{570} over a time scale of milliseconds (Xie et al., 1987). The retinal is covalently bound to K216 of the protein via a protonated Schiff base. In the L→M reaction, the Schiff base proton is transferred to the internal acceptor D85 on the proton release side (Engelhard et al., 1985; Braiman et al., 1988a; Gerwert et al., 1989; Fahmy et al., 1992). M is the only photocycle intermediate containing a deprotonated Schiff base and therefore has a far blue-shifted absorption maximum as compared to the other intermediates and to the ground state BR_{570}. This allows an unperturbed monitoring of the rise and decay of M_{410} in the blue spectral region. During the following M→N reaction, the Schiff base regains a proton from the internal proton donor D96, located on the proton uptake side (Gerwert et al., 1989, 1990a; Pfefferlé et al., 1991; Bousché et al., 1991). Reprotonation of the Schiff base shifts the absorption maximum back to the green in N_{530}. In the $N_{530} \rightarrow O_{640}$ transition, the chromophore reisomerizes to all-*trans*-retinal (Smith et al., 1983). The absorption maximum is far red-shifted because the counterion D85 is still protonated (Souvignier and Gerwert, 1992).

Several photocycle models have been suggested. Originally, a linear sequence of unidirectional reactions was proposed (Lozier et al., 1975). This scheme, however, cannot account for the observed biphasic rise and decay of M (Xie et al., 1987). To explain this complex kinetic behavior, a multitude of different photocycle models have been postulated; for a recent review see Lanyi and Váró (1995) and the citations therein. The proposed models vary between two extremes: 1) parallel photocycles originating from different BR_{570} ground states and 2) a linear sequence with significant back-reactions. In addition, several authors propose the existence of two different M intermediates, designated as M_1 and M_2 (e.g., Váró and Lanyi, 1991a,b, and citations therein). In the $M_1 \rightarrow M_2$ transition the deprotonated Schiff base should change its orientation from the internal proton acceptor D85 on the proton release side in M_1 to the internal proton donor D96 on the proton uptake side in M_2. The accessibility change of the central proton binding site, the Schiff base, from the proton release side in M_1 to the proton uptake side in M_2 may be responsible for the directionality of the pump. There are at least two different possible explanations for this "reprotonation switch" at the molecular level: either the chromophore reorients the Schiff base by a single bond isomerization around the C_{14}-C_{15} retinal bond from the proton release to the proton uptake side (Schulten and Tavan, 1978; Gerwert and Siebert, 1986), or a different orientation of the peptide

Received for publication 22 July 1996 and in final form 21 July 1997.

Address reprint requests to Dr. Klaus Gerwert, Lehrstuhl für Biophysik, Fakultät Biologie, Ruhr Universität Bochum, 44780 Bochum, Germany. Tel.: +49-234-700-4461; Fax: +49-234-709-4238; E-mail: gerwert@helios.bph.ruhr-uni-bochum.de.

0006-3495/97/10/2071/10 $2.00

backbone induces a change in the Schiff base accessibility (C-T model; Fodor et al., 1988).

The existence of multiple M substates has been excessively investigated. An analysis, based on time-resolved visible absorption spectroscopy, has shown that the absorbance changes can be described in the framework of a sequential model, including two M substates with the same visible absorption maxima (Váró and Lanyi, 1991a,b). However, M substates, which are only kinetically different, as proposed by photocycle modeling, can also be explained by parallel photocycle models. The problem is experimentally underdetermined, because the number of experimentally accessible apparent rate constants is smaller than the number of microscopic rate constants describing the individual photocycle reactions. Therefore many photocycle models can fit the data. Nevertheless, two sequential M substates with slightly different absorption maxima in the visible have been identified in monomeric bR as well as in D96N mutant protein (Váró and Lanyi, 1991a; Zimányi et al., 1992). In D96N, for example, the maximum of an early M (412 nm) corresponds to that of the wild-type M, whereas that of the late M is blue-shifted to 404 nm. The 8-nm shift in the mutant protein might be explained by the Schiff base orientation in M_2 to the cytoplasmic side, at which D96 has been changed to N96 (Zimányi et al., 1992).

Distinct M substates, differing in the conformational state of the protein backbone, have been suggested on the basis of vibrational spectroscopy (Ormos, 1991; Perkins et al., 1992). However, the observed differences in the M-like spectra were later attributed to the presence of a significant amount of the N spectrum superimposed on M (Ormos et al., 1992; Hessling et al., 1993). In another approach, time-resolved absorbance changes were measured simultaneously in the infrared and visible spectral ranges and analyzed by factor analysis and decomposition (Hessling et al., 1993). This analysis deconvolutes the absorbance changes in the visible and the infrared into the pure difference spectra without assuming a specific photocycle model (Malinowski, 1980). However, even though the analysis was capable of determining an M spectrum without contamination by those of the other intermediates, it does not resolve two spectroscopically different M substates in the wild type. Because this method can separate only spectroscopically and kinetically distinct intermediates that are significantly accumulated, two spectroscopically very similar M substates could have been merged.

The problem of resolving kinetically and spectroscopically overlapping intermediates can be circumvented by utilizing the photo-back-reaction of photocycle intermediates (for a recent review see Balashov, 1995). Photoconversion of the M intermediate at low temperatures leads to a series of transitions that can be summarized by the scheme $M \rightarrow M' \rightarrow BR' \rightarrow BR$. The primary reaction $M \rightarrow M'$ was attributed to a 13-*cis*→all-*trans* isomerization of the retinal (Kalisky et al., 1977; Hurley et al., 1978). At liquid nitrogen temperatures, two different photoproducts of M are found, which decay into a long-wavelength species (BR′). On the basis of the low-temperature data alone, it is not possible to decide whether these correspond to different M substates. The $M' \rightarrow BR'$ transition has been interpreted in terms of Schiff base reprotonation (Takei et al., 1992).

The most convincing experimental evidence of a heterogeneous M population was obtained through studies of M photo-back-reaction at room temperature (Druckmann et al., 1992, 1993). In this analysis the photocycle was initiated by a green laser pulse followed by a delayed blue pulse that selectively drives the M photo-back-reaction. Because the apparent rate of the Schiff base reprotonation in the $M' \rightarrow BR'$ transition depends on the delay between the two pulses, two different oriented M′ and thus two consecutive precursors, termed M_1 and M_2, are suggested, with different proton accessibilities to the Schiff base. These experiments imply a time constant of ~100 μs for the $M_1 \rightarrow M_2$ transition. Nevertheless, these experiments yield only kinetically distinct but not spectroscopically different M substates. Here we have utilized this approach in the infrared spectral region, which gives information about the protein and the chromophore reactions at the atomic level. We use step-scan Fourier transform infrared (FTIR) spectroscopy with 30-ns time resolution (Uhmannn et al., 1991; Weidlich and Siebert, 1993; Plunkett et al., 1995; Hage et al., 1996; Rammelsberg et al., 1997). After the photocycle is initiated with a green laser pulse, a delayed blue laser pulse selects an early or late appearing M, depending on the delay time. This procedure permits the determination of BR-M_1 and BR-M_2 difference spectra without contribution from other intermediates. The IR spectra allow conclusions about the molecular mechanism of the reprotonation switch to be drawn.

MATERIALS AND METHODS

Wild-type bacteriorhodopsin was purified from *H. salinarium* as purple membrane sheets according to a standard method (Oesterhelt and Stoeckenius, 1974). Suspensions of bR with 500 mM HEPES/Tris and KCl, as indicated in the figure legends, were pelleted and squeezed between two CaF_2 windows separated by a polyethylene spacer of 2.5-μm thickness. The sample was then positioned in a temperature-controlled home-built sample chamber.

Step-scan FTIR spectroscopy was performed on a Bruker IFS 66V spectrometer mounted on a vibrationally decoupled table (RS 3000; Newport). We calculated the residual fluctuations of the stabilized movable mirror to be smaller than ±2 nm.

Two types of IR detectors were used. Detected signals of a standard MCT photoresistance (Graseby) with a two-stage preamplifier (detector rise time 5 μs) were converted (16-bit ADC, 200 kHz) and Fourier-transformed with the Bruker spectroscopy software OPUS. In addition, a photovoltaic MCT detector (Kolmar) with a home-built preamplifier (rise time 30 ns) with DC and AC outputs was used. The DC output was fed to the standard 16-bit/200-kHz ADC, and the AC output was connected to a 200-MHz/8-bit analog-digital converter (PAD 82; Spektrum). Both detectors were cooled to 77 K with liquid nitrogen. The spectral range was limited to 1950 cm^{-1} via an interference filter. All spectra were taken with a spectral resolution of 4 cm^{-1}.

In step-scan spectroscopy the movable mirror is kept stationary while the respective process is initiated, and the time dependence of the infrared intensity at the interferogram sampling position is recorded. After completion of the reaction (i.e., after relaxation of the sample), the mirror is moved stepwise to the next sampling position of the interferogram. As such, the

time course of each point of the interferogram is determined. Thereby the time resolution is not restricted by the mirror velocity but only by the detector rise time. The calculation of spectral absorbance changes $\Delta A(t, \nu)$ follows, in principle, the procedure described in Uhmann et al. (1991). It differs, however, in the acquisition of the phase function $\phi(\nu)$ due to a modified acquisition software. For a more detailed description of the procedures applied, see Rammelsberg et al. (1997).

Before and after each step-scan measurement, the sample is checked by a standard fast-scan measurement to ensure that no significant change of hydration or denaturation of the sample has occurred. Throughout the whole step-scan measurement, absorbance changes were simultaneously detected in the visible as an independent measurement of the amount of BR photocycling and the amount of the M intermediate driven back to BR. This procedure also checks the stability of the exciting laser energy.

Excitation of the sample is achieved by two dye lasers pumped by two excimer laser systems (LPX 240i/LPX 300; Lambda Physik). Coumarin 153 dye (maximum 540 nm) initiates the photocycle, and a blue emitting dye (PBBO, 400 nm) drives the M photo-back-reaction. The triggering of the lasers as well as the time delay Δt are controlled by a home-built delay/trigger unit. A weak reflex of the laser pulse hits a fast photodiode, which starts the infrared data acquisition.

The BR-M_1 and BR-M_2 difference spectra are obtained in the following way (also see Scheme 1). Time $t = 0$ represents the onset of the first green laser pulse (pulse duration 20 ns). After a delay time Δt, a second blue pulse (pulse duration 20 ns) is applied to the sample. The delayed second pulse results in a partial depletion of the M state(s) due to its photo-back-reaction. Calculating a difference $\Delta\Delta A$,

$$\Delta\Delta A = \Delta A(t_1) - \Delta A(t_2)$$

between absorbance changes $\Delta A(t_1)$ at the time t_1 just before the second pulse is applied, and $\Delta A(t_2)$ at the time t_2 at which the M photo-back-reaction is completed, yields mostly a BR-M difference spectrum. Double difference spectra (shown in Fig. 4) are calculated as indicated in Fig. 2. For an enhanced signal-to-noise ratio we averaged 50 absorbance difference spectra before and after the second flash to calculate $\Delta A(t_1)$ and $\Delta A(t_2)$, respectively (Fig. 2). The difference spectra are taken every 10 ns, that means 500 ns before and 500 ns after the flash is averaged. Here the time interval $[t_1;t_2]$ was chosen to be as short as 1.5 μs to minimize the effect of continuing photocycle reactions that are superimposed on the photo-back-reaction of M. In particular, the decay of the L intermediate to M with a half-time of ~50 μs has to be considered during this period of time. The contribution of thermal interconversion of photocycle intermediates was therefore investigated in another, parallel measurement, performed under identical conditions but in the absence of a second pulse (*continuous line* in Scheme 1). Here the double difference $\Delta\Delta A$, calculated as before, accounts only for thermal photocycle reactions in the time period between t_1 and t_2. Spectra presented in Fig. 4 were corrected by the subtraction of the estimated superposition of the photocycle from the double difference of the two-pulse experiment. This procedure neglects the fact that in addition to the normal photocycle reactions, the L ↔ M and the M ↔ N equilibria are changed because the blue flash depopulates the M intermediate. Using a time interval of 10 μs between $\Delta A(t_1)$ and $\Delta A(t_2)$ gave significant L contributions to the difference spectra, indicated by an ethylenic band at 1556 cm^{-1}. Nevertheless, over a time interval of 1.5 μs, this band disappears, and therefore effects due to the M depletion seem to be negligible.

Finally, the photocycle initiation of the blue laser must be considered. We have determined this contribution by a control experiment. Application of the blue pulse alone drives only ~5% of the bR molecules into the photocycle as compared with the green pulse. Nevertheless, because a significant repopulation of the ground-state BR is not expected within the longest delay Δt used (<500 μs), the contribution of this blue-excited photocycle does not depend on the respective delay and is therefore constant for all difference spectra.

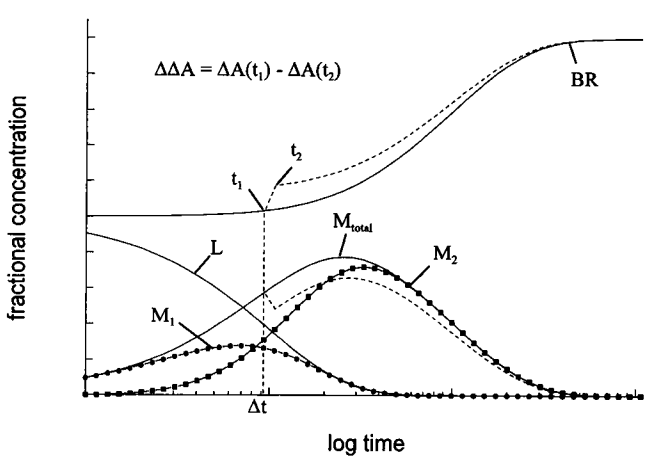

Scheme 1 Transient intermediate concentration based on a simplified model of the photocycle (L→M→BR), illustrating the procedure of double difference calculation. Continuous lines indicate the expected time course in a single pulse experiment, whereas dashed lines refer to a double pulse experiment. The total M-concentration M_{total} is reduced to its fractional components M_1 (●) and M_2 (■), as implied by double-pulse experiments in the visible (Druckmann et al., 1992).

RESULTS

The basic idea of our experiments is illustrated in Scheme 1. A time course of L, M_{total}, and BR concentrations as yielded by a simplified unidirectional model, L→M_{total}→BR ($k_{L\to M}/k_{M\to BR}$ = 10/1), is shown. In addition, the proposed contributions of M_1 and M_2 to M_{total} as obtained by photocycle modeling (Váró and Lanyi, 1991a) and double-flash experiments (Druckmann et al., 1992) are also illustrated in Scheme 1. These calculations suggest that M_1 comprises most of the total M during the M rise, and M_2 comprises most of the total M when M reaches its maximum concentration. At time $t = 0$, the photocycle is initiated by a green laser flash. After a delay time Δt, the application of a second blue pulse selectively drives only the bR molecules in the blue-absorbing M intermediate back to BR. The M to BR photo-back-reaction is illustrated by a decreasing M concentration and an increasing BR concentration. The L concentration is not affected in such a simplified scheme without back-reactions. The photo-back-reaction of M starts at t_1 and is completed at t_2. It is found to be considerably faster (~200 ns; Kalisky et al., 1977) than thermal reactions of the photocycle (L ↔ M, ~100 μs; M ↔ N, ~ms). Thus we can discriminate kinetically between changes due to the fast M→BR photo-back-reaction and the slower photocycle reactions such as L ↔ M_1 or M_2 ↔ N. The BR molecules that are not photo-back-reacted decay in the conventional photocycle. By calculating double-difference spectra between the absorbance changes at t_1 (M concentration higher) and t_2 (M concentration lower), only the absorbance changes due to the M to BR photo-back-reaction are selected. That is, a BR-M difference spectrum is obtained. Because the results of the simple photocycle modeling and the double-flash experiments show that at shorter delay times Δt M_1 dominates and at later delay times M_2 dominates, the BR-M_1 and

BR-M_2 difference spectra can be obtained by variation of the delay time Δt.

Fig. 1 shows typical results of a measurement at pH 6.5 and 20°C, performed with a time resolution of 5 μs. Three traces at 1762 cm^{-1} and 1527 cm^{-1}, respectively, obtained with three different delay times Δt (70 μs, 150 μs, and 250 μs), are superimposed. The absorbance change over a time interval of only 1 ms is plotted. Data collection started 20 μs before the application of the first pulse. The absorbance increase at 1762 cm^{-1} indicates the protonation of D85 and reflects the accumulation of the total M concentration (Hessling et al., 1993). The absorbance decrease at 1527 cm^{-1} refers to the disappearance of the BR ground state. The traces depicted indicate that the application of the delayed blue pulse results simultaneously in a fast unresolved depletion of the M intermediate and in the reappearance of the ground-state BR. Obviously, only part of the accumulated M reacts back to BR. Until the maximum concentration of M is reached, the longer the delay before the second pulse, the more M is accumulated and the more the second pulse depopulates M. This observation for M agrees with the increasing repopulation of BR with increasing Δt. On the other hand, photocycle intermediates that are not affected by the second pulse continue to react as usual. Therefore, the M concentration increases again after application of the blue pulse because, before the time of the maximum M concentration, the decay of the unaffected L intermediate is faster than M decay to N. The contribution of the photocycling bR induced by the blue pulse can be neglected under the conditions used, as discussed in Materials and Methods.

To resolve the M→BR back-reaction, the same experiments were performed with 30-ns time resolution. In a first experiment the second pulse was delayed long enough (Δt = 350 μs) to coincide with the maximum of the total M concentration. In a second experiment with the same sample, the two pulses were separated by only 50 μs, thereby monitoring the photo-back-reaction of the early M population. The corresponding absorbance changes are shown in Fig. 2. Data acquisition starts 500 ns before the application of the second pulse. A time interval of 3.5 μs is shown. The

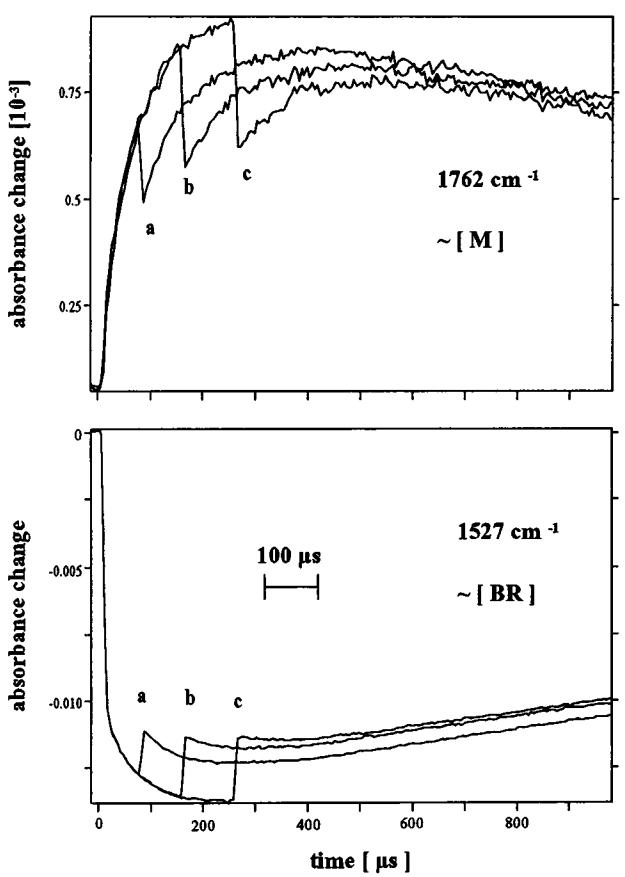

FIGURE 1 Absorbance change in the infrared at 1762/1527 cm^{-1}, where M/BR concentration is followed (pH 6.5, 500 mM HEPES/KCl). Three measurements with delay times of (*a*) 70 μs, (*b*) 150 μs, and (*c*) 250 μs are superimposed (t = 0 represents initiation of the photocycle by the first laser pulse). The amount of M intermediate photoconverted obviously depends on the already accumulated M.

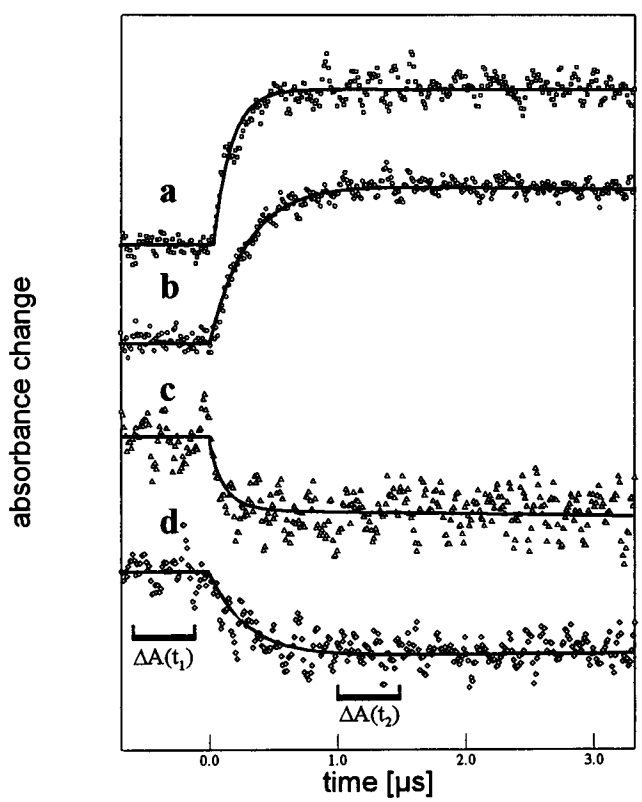

FIGURE 2 Absorbance changes in the infrared measured with a time resolution of 30 ns (pH 7.5, 500 mM Tris/KCl). Only a time interval of 4 μs during the back-photoreaction of M is printed. (Note: here t = 0 represents the application of the second pulse.) Traces were analyzed with the global-fit algorithm by a single exponential function (*continuous line*). Double differences were calculated from the average of spectra measured within a time interval of 500 ns before and after back-photoreaction, as indicated by brackets. (*a*) Absorbance changes at 1527 cm^{-1}, Δt = 50 μs. (*b*) 1527 cm^{-1}, Δt = 350 μs. (*c*) 1762 cm^{-1}, Δt = 50 μs. (*d*) 1762 cm^{-1}, Δt = 350 μs. The amplitude of the detected signal corresponds to an absorbance change of 3.4×10^{-3} (*a*), 4.8×10^{-3} (*b*), 3.7×10^{-4} (*c*), and 5.4×10^{-3} (*d*), respectively.

recovery of BR at 1527 cm^{-1} and the depletion of M at 1762 cm^{-1} can now be followed as a function of time. Global-fit analysis of the spectral range from 1800 cm^{-1} to 1000 cm^{-1} succeeds with a single exponential function (*continuous lines* in Fig. 2) and reveals apparent time constants of $0.8 \times 10^7\ s^{-1}$ (Δt = 50 μs) and $0.36 \times 10^7\ s^{-1}$ (Δt = 350 μs), respectively. Please note that this a result of a fit procedure applied simultaneously to 400 spectral elements, individually weighted with respect to the calculated noise at each wavelength. This leads to a significant improovement of the calculated rate constants (Hessling et al., 1993). Similar time constants ($k_{M1} = 1.0 \times 10^7\ s^{-1}$; $k_{M1} = 0.4 \times 10^7\ s^{-1}$) of the M photo-back-reaction depending on the delay times have been observed in the visible spectral range (Druckmann et al., 1992) and are now confirmed in the infrared. After completion of these processes, the exemplary traces shown in Fig. 2 reveal no significant further absorbance change due to the photocycle reactions of the unaffected intermediates. Thus we conclude that in this time domain no photocycle reactions interfere.

To determine the absorbance changes during the $M_1 \rightarrow M_2$ transition, we calculate differences between the time-resolved absorbance difference spectra taken before the application of the second pulse at t_1 and after completion of the M back-reaction at t_2 (see also Fig. 2). Fig. 3 *a* shows the resulting double-difference spectrum BR-M of the late M intermediate (t_{res} = 30 ns, Δt = 350 μs, pH 7.5, 25°C). It is compared to the BR-M spectrum (Fig. 3 *b*) yielded by factor analysis from a conventional single-flash, time-resolved measurement (Hessling et al., 1993). General agreement is found, especially for the M typical bands at 1762 cm^{-1} and the band pattern at 1214 cm^{-1}, 1201 cm^{-1}, and 1167 cm^{-1}. A considerable deviation is seen at 1634 cm^{-1}. This band seems to be downshifted from 1641 cm^{-1} in Fig. 3 *b*, or a positive band appears at 1641 cm^{-1}. The band at 1641 cm^{-1} represents the C=NH^+ stretching vibration in the BR ground state (Smith et al., 1987). A further deviation is seen at 1660 cm^{-1}. Furthermore, a small negative band at 1700 cm^{-1} is missing in the double-flash difference spectrum. Because there are some small but significant deviations between the two difference spectra, we designate the double-flash difference spectrum as the "photo-back BR-M spectrum" to differentiate it from the time-resolved BR-M spectrum.

Several double-flash experiments were performed between pH 7 and pH 9, and these revealed a similar delay dependence of the absorbance changes in the M photo-back-reaction. As a typical result, the BR-M difference spectra obtained with a sample at pH 7.5 are depicted in Fig. 4. Here we compare the photo-back BR-M spectrum, measured with a delay Δt of 350 μs (Fig. 4 *a*), to the photo-back BR-M spectrum at Δt = 50 μs (Fig. 4 *b*). As discussed above, the one at shorter delay represents mostly a BR-M_1 difference spectrum and the other a BR-M_2 difference spectrum. When considering the delay dependence of the M photo-back-reaction in the visible spectral range (Druckmann et al., 1992) at Δt = 50 μs, we expect ~80% of the total amount of M to be in the M_1 state, and at Δt = 350 μs, we expect 100% to be in M_2. Nevertheless, a more exact decomposition to M_1 and M_2 on the basis of infrared data cannot be given.

No large differences are seen between the BR-M_1 and BR-M_2 difference spectra. In particular, the chromophore bands in the fingerprint region (1254 cm^{-1}, 1200 cm^{-1}, 1166 cm^{-1}), the ethylenic stretch difference band (1567 cm^{-1}, 1527 cm^{-1}), and the absorbance changes of the carboxyl groups (1761 cm^{-1}, 1738 cm^{-1}) are in good agreement. Nevertheless, deviations are seen at 1687 cm^{-1}, 1660 cm^{-1}, 1641 cm^{-1}, 1634 cm^{-1}, and 1276 cm^{-1}. The deviation at 1687 cm^{-1} is less significant. At 1641 cm^{-1}, the band intensity decreases with larger delay times but increases at 1634 cm^{-1} and 1660 cm^{-1}. In addition, there is

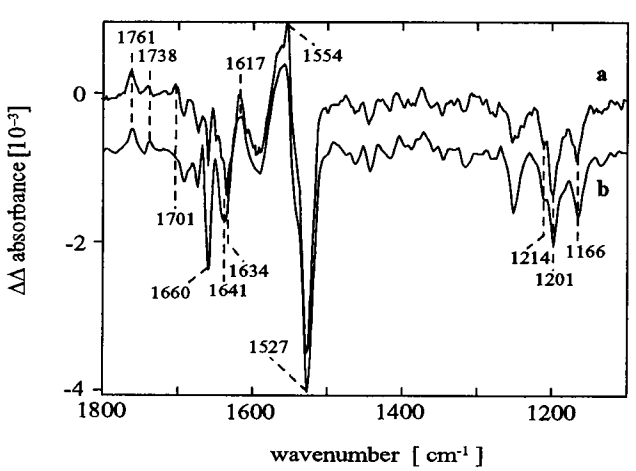

FIGURE 3 Comparison of (*a*) a late photo-back M-spectrum out of a time-resolved double-pulse experiment (time resolution: 30 ns, pH 7.5, 25°C, Δt = 350 μs) to (*b*) the single pulse time-resolved M-spectrum calculated with factor analysis (Hessling et al., 1993).

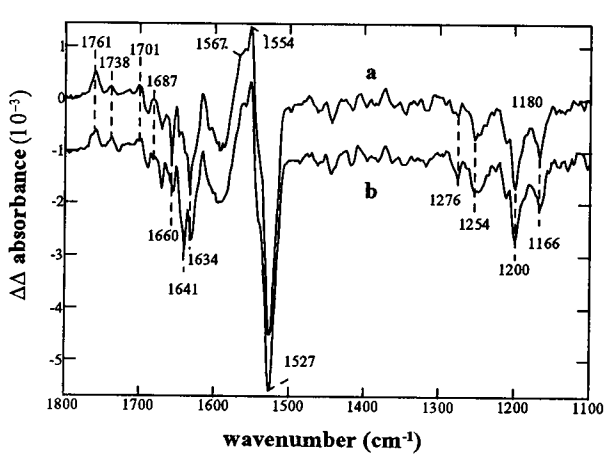

FIGURE 4 Photo-back BR′-M spectra obtained at Δt = 350 μs (*a, upper spectrum*) and at Δt = 50 μs (*b, lower spectrum*) (pH 7.5, 500 mM Tris/KCl). The lower spectrum represents mainly a BR_1'-M_1, and the upper spectrum a BR_2'-M_2 difference spectrum. Spectrum *b* is magnified by a factor of 1.4 for comparison.

a significant absorbance increase at 1276 cm^{-1} in the photo-back BR-M_2 spectrum.

We have also performed double-flash experiments with a deuterated sample. However, in contrast to the H_2O experiment, no delay-time dependence of the double-difference spectra was found. This observation can be explained in the framework of a model in which the $L \rightarrow M_1$ transition is selectively slowed down by a factor of ~6 in the deuterated samples, but where the time constant of the $M_1 \rightarrow M_2$ transition is only slowed down by a factor of 1.5 (le Coutre and Gerwert, 1996). Then no significant accumulation of M_1 would occur.

Fig. 5 shows the BR-N difference spectrum as revealed by factor analysis (Hessling et al., 1993) for comparison purposes. The most prominent bands of the N intermediate are the shifted carbonyl frequency of D85 at 1755 cm^{-1}, a pronounced difference band pair at 1670/1650 cm^{-1} (−/+) in the amide I region, and the increased absorption at 1183 cm^{-1} that indicates a reprotonated Schiff base in N. It is obvious from the comparison with the photo-back BR-M difference spectra in Fig. 4 that the absorbance changes in the amide I and amide II regions in the M→N transition are clearly distinct from the absorbance changes observed in the $M_1 \rightarrow M_2$ reaction.

DISCUSSION

The double-flash experiments resolve two different M intermediates in the infrared spectral region. The second flash induces a reaction pathway according to M→M′→BR′→BR, in which the deprotonated Schiff base retinal isomerizes from 13-*cis* to all-*trans* in the M→M′ reaction, the Schiff base is reprotonated in the M′→BR′ reaction, and the protein relaxes to its ground state in the BR′→BR reaction. The M→M′ reaction takes place most likely in the picosecond time range and is not time resolved in our study.

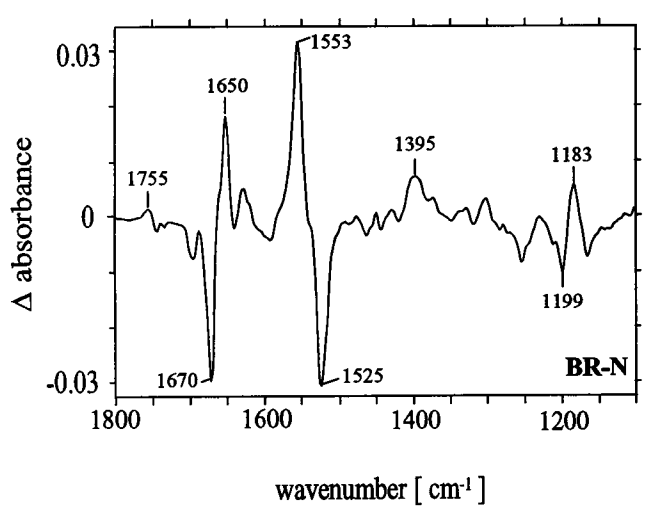

FIGURE 5 The BR-N spectrum from factor analysis (Hessling et al., 1993), illustrating strong absorbance differences in the amide I region (1670/1650 cm^{-1}).

But we resolve the reprotonation of the Schiff base. Because in the photoinduced back-reaction of an early-appearing M (short delay times) the Schiff base reprotonates in 86 ns ($k_{M1} = 0.8 \pm 0.1 \times 10^7\ s^{-1}$), but in the late appearing M (long delay times) it reprotonates in 192 ns ($k_{M2} = 0.36 \pm 0.05 \times 10^7\ s^{-1}$), we conclude that the proton accessibility of the Schiff base in the two M states is different. In the early-appearing M, the Schiff base may be connected to the proton release side, whereas in the late-appearing M it may be connected to the proton uptake side. In this case it represents part of the reprotonation switch. The results agree nicely with the two rate constants observed earlier in the visible spectral range ($k_{M1} = (1 \pm 0.2) \times 10^7\ s^{-1}$, $k_{M2} = (0.4 \pm 0.1) \times 10^7\ s^{-1}$; Druckmann et al., 1992).

Negative bands in the difference spectra characterize the BR state and positive bands the M state. The late photo-back BR-M difference spectrum deviates with respect to the BR bands from the BR-M difference spectrum obtained by factor analysis at 1641 cm^{-1} and 1660 cm^{-1} (Fig. 3). The band at 1660 cm^{-1} may represent an amide I vibration, indicating a slightly different peptide bond orientation involving one or two bonds. The band at 1641 cm^{-1} characterizes the C=NH^+ vibration. Because the difference spectra agree mostly regarding BR-bands and deviate for the C=NH^+ vibration, it seems that specifically the microenvironment of the Schiff-base is different, but the opsin and the chromophore have almost reached the BR ground-state configuration. The deviations indicate that we observe not the BR state but the precursor, BR′. The final BR′→BR relaxation reaction seems to take place on a longer time scale than is monitored in this study. Therefore the photo-back BR-M spectra represent BR′-M difference spectra.

Furthermore, the comparison of the photo-back BR′-M spectra with the BR-M spectrum obtained by factor analysis does not show the negative BR band at 1700 cm^{-1}, but a positive band (Fig. 3). The band at 1700 cm^{-1} is assigned to E204 (Brown et al., 1995), but the assignment to E204 has recently been ruled out (Huhn et al., manuscript submitted for publication). It is not clear which group is actually represented by this band. Nevertheless, the absence of this band may indicate that a proton is released from the protein in the L→M transition but not yet regained in BR′. Future experiments with indicator dyes should clarify this question.

It is shown, furthermore, that in the M′→BR′ reaction the Schiff base is reprotonated by D85 because its reprotonation kinetics, followed at 1527 cm^{-1}, agrees nicely with the deprotonation kinetics of D85, followed at 1762 cm^{-1}. This result of the time-resolved experiments agrees with the conclusion drawn from a static low-temperature FTIR study (Takei et al., 1992).

Low-temperature studies of the M photo-back-reaction (Balashov and Litvin, 1981) indicate that the Schiff base reprotonation is followed by a series of thermal transitions via distinct intermediates P565, P575, and P585 observed by a gradual warming of the sample. In principle, these intermediates could show up at room temperature as well. Only P585 is expected to decay at room temperature in the

microsecond to millisecond time range; it may represent BR′. For such a red-shifted intermediate, a frequency downshift of the ethylenic vibration of ~4 cm^{-1} is expected because of the relationship between the IR frequency and the wavelength of the visible absorption maximum. However, such frequency shifts are not observed in the room-temperature BR′-M photo-back difference spectra (see Fig. 3). Thus P585 does not contribute to the photo-back BR′-M spectra at room temperature.

In comparing the BR_1'-M_1 and BR_2'-M_2 difference spectra with each other, only very few deviations are observed. This is not surprising, because the factor analysis was not able to resolve two different M intermediates. Therefore it was proposed that the spectral deviations between M_1 and M_2 may only be minute. The BR_1'-M_1 and BR_2'-M_2 difference spectra deviate at 1687, 1660, 1641, 1635, and 1276 cm^{-1}. The band at 1276 cm^{-1} is assigned to the C-O^- stretching vibration of Y185 in the ground state by combining FTIR difference spectroscopy with side-directed mutagenesis (Braiman et al., 1988b). It is down-shifted to 1272 cm^{-1} in the M intermediate. Interestingly, this study has also observed a shift in the BR C=NH^+ stretching vibration in the Y185F mutant to 1634 cm^{-1} in low-temperature BR-K and BR-M difference spectra. A close electrostatic interaction of the ionized Y185 with the positively charged Schiff base in the wild type was concluded from these results. Different hydrogen bonding of the Schiff base proton led to significant shifts in the C=NH^+ stretching frequency in BR_1' and BR_2', in analogy to a recent investigation on human visual pigments (Kochendoerfer et al., 1997). The assignment of the absorbance changes at 1276 cm^{-1} to a vibration of Y185 was confirmed in side-directed isotopic labeling studies (Liu et al., 1995). However, it should be noted that UV resonance Raman as well as solid-state NMR experiments do not support the presence of a tyrosinate in the BR ground state (Herzfeld et al., 1990; McDermott et al., 1991; Ames et al., 1992). It might be that because of the different time scales resolved by the infrared and NMR spectroscopy, a fast fluctuating proton is averaged in the NMR experiments and might reflect only a fractional ionization of Y185 (Liu et al., 1995). A recent electron-crystallographic refinement of the bacteriorhodopsin structure indicates that Y185 could be hydrogen-bonded to D212, which is part of the complex counterion of the Schiff base (Grigorieff et al., 1996). However, the simultaneous spectral deviation at 1276 cm^{-1} and 1641 cm^{-1} between the BR_1'-M_1 and BR_2'-M_2 difference spectra reflect changes in the Schiff base/Y185 interaction with the M_1 to M_2 transition, either in the protonated or in the deprotonated form of Y185.

Further changes are seen at 1687 cm^{-1}. In a recent study on wild-type and R108Q mutated halorhodopsin, a difference band at 1695/1688 cm^{-1} is assigned to the frequency shift of the R108 guanidino group (Rüdiger et al., 1995). The arginine at position 108 in halorhodopsin is homologous to R82 in bacteriorhodopsin. Therefore the small deviations at 1687 cm^{-1} in the BR-M_1 and BR-M_2 difference spectra may indicate different orientations of R82 in the different M states, as has recently been suggested (Bashford and Gerwert, 1992; Scharnagl et al., 1995; Sampogna and Honig, 1996). Nevertheless, a clear-cut assignment needs future studies with R82X mutated bR.

Because no deviations of the chromophore's vibrational bands of the M intermediate are seen in the BR-M_1 and BR-M_2 difference spectra, especially in the fingerprint region, there is no evidence of a change in the retinal conformation, such as a C_{14}-C_{15}-s-*cis* in M_1 to s-*trans* in M_2. It was suggested that the C_{14}-C_{15} single-bond isomerization may constitute the reprotonation switch (Schulten and Tavan, 1978). Nevertheless, in M the chromophore is deprotonated and has weak infrared intensities. Therefore, small differences in the chromophore isomerization state may not be indicated in the BR_1'-M_1 and BR_2'-M_2 difference spectra (Schulten et al., 1984; Xu et al., 1995). In addition, the comparison of the L and N Raman spectra, which should contain a 14-s-*cis* and a 14-s-*trans*, respectively, show a nice agreement of the chromophore vibrations in the fingerprint region (Eisfeld et al., 1993; Hessling and Gerwert, unpublished results). This suggests that L and N share a very similar chromophore conformation, and thus in the $M_1 \rightarrow M_2$ transition no significant chromophore structural change seems to take place.

Comparison of the spectral changes in the $M_1 \rightarrow M_2$ transition to the ones in the BR-N difference spectrum (Fig. 5) from factor analysis (Hessling et al., 1993) reveals considerable deviation. The BR-N difference spectrum is dominated by a strong difference band at 1670/1650 cm^{-1} and a strong band at 1553 cm^{-1}. They indicate a structural movement of three or four peptide backbone bonds (Hessling et al., 1993). These absorbance changes are not seen in the $M_1 \rightarrow M_2$ transition. Instead, a negative band at 1660 cm^{-1} appears, which may represent a peptide bond movement of another bond. Thus we propose two consecutive peptide bond movements: first, a minute one in the $M_1 \rightarrow M_2$ transition, which turns the Schiff base accessibility from the proton release to the proton uptake side; second, a larger one in the $M_2 \rightarrow N$ transition. The second one may be induced by the rise of a negative charge at D96 in the proton uptake side. The structural changes monitored in the neutron and electron diffraction studies (Koch et al., 1991; Subramaniam et al., 1993) reflect mainly this second, larger structural change, because the investigators trapped an M_N (Sasaki et al., 1992). In the D96N mutant the protein is trapped in the wild-type protein backbone N configuration in M_N. The structural changes identified so far by neutron and electron diffraction studies do not reflect the reprotonation switch in the $M_1 \rightarrow M_2$ transition, but rather the opening of the protein for the proton uptake by D96 in N.

Based on the obtained results, we propose the following model (see Scheme 2): after initiating the photocycle with a first laser flash, a second blue flash drives a 13-*cis* retinal Schiff base to all-*trans* in the M→M′ transition. At an early stage of M, mostly M_1 is driven to M_1', whereas at a late stage of M, M_2 is driven to M_2'. The M_1 to M_2 transition seems to take place in ~100 μs. The Schiff base has

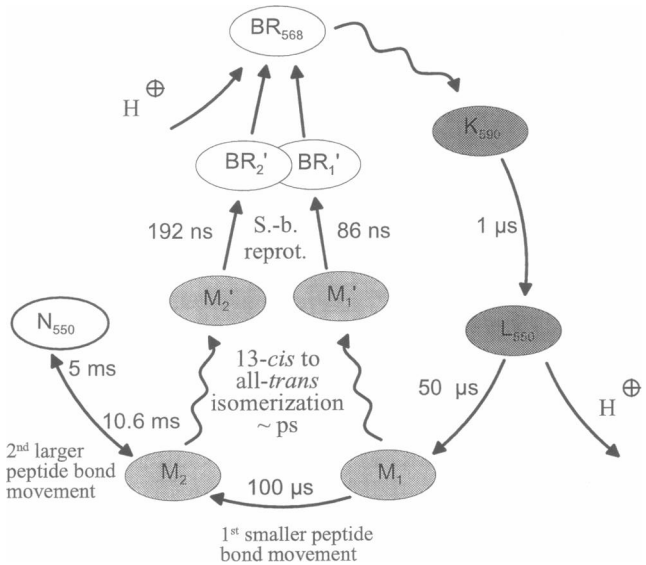

Scheme 2 Refined photocycle model considering the results of double-pulse experiments in the infrared spectral region. A first protein conformational change during the fast M_1 to M_2 transition reorients the Schiff base to the cytoplasmic side. In a second and larger conformational change, probably triggered through D96 deprotonation, the intermediate N is formed. For more details see text.

different proton accessibilities, in the M_1 configuration to the external proton release pathway, and in the M_2 configuration to the cytoplasmic proton uptake pathway. The different proton accessibilities lead to different reprotonation rate constants observed for the $M_1 \rightarrow BR'_1$ and $M_2 \rightarrow BR'_2$ transition. The BR′ also seems to reflect different oriented protein states. The spectral deviations seen at 1641 cm^{-1} and 1276 cm^{-1} reflect different interactions of the Schiff base with Y185 in BR'_1 and BR'_2, and conclusively in M_1 and M_2. Different H-bonding shifts the $C{=}NH^+$ frequency down to 1634 cm^{-1} in BR'_2, as compared to 1641 cm^{-1} in BR'_1. There is experimental evidence for complex H-bonded networks in the proton release and proton uptake pathway, respectively (le Coutre et al., 1995; le Coutre and Gerwert, 1996; Huhn et al., manuscript submitted for publication). The results indicate that in the $M_1 \rightarrow M_2$ transition, mostly the H-bonding of the Schiff-base is changed, presumably from the proton release H-bonded network to the proton uptake H-bonded network. Large-scale structural changes are not observed. The movement leading to the different H-bonding of the Schiff base to Y185 is indicated by the band at 1660 cm^{-1}, which seems to represent a small peptide bond movement and the band at 1687 cm^{-1}, which may indicate different R82 conformations. Further experiments are needed to clarify those band assignments. In summary, the reprotonation switch in the M_1 to M_2 transition is essentially performed by different H-bonding of the Schiff base to Y185, most likely induced by minute peptide bond movements leading to different proton accessibilities. In the $M_2 \rightarrow N$ transition, a structural change four to five times larger is seen. The structural changes in the amide I region may indicate a movement of helix F, using the Y185-P186 peptide bond as a hinge to open the cytoplasmic proton uptake pathway for proton access (Gerwert et al., 1990b).

In summary, we have for the first time combined FTIR spectroscopy with double-flash experiments to obtain structural information about photocycle intermediates. This successful combination opens up the possibility of using multiple laser pulses or other pulse excitations to create artificial photocycles for light-sensitive molecules that can be driven back into their ground state by a short excitation pulse. This now opens a window for slecting, by nanosecond FTIR spectroscopy, from a mixture of different protein states, the IR spectrum of one specific intermediate that is contaminated with contributions of the other intermediates in conventional time-resolved measurements.

The authors thank Dr. David Rumschitzki for critical reading of the manuscript and for correcting the English.

Financial support of the Deutsche Forschungsgemeinschaft (SFB 394, Teilproject C2) is gratefully acknowledged.

REFERENCES

Ames, J. B., M. Ros, J. Raap, J. Lugtenburg, and R. A. Mathies. 1992. Time-resolved ultraviolet resonance Raman studies of protein structure: application to bacteriorhodopsin. *Biochemistry.* 31:5328–5334.

Balashov, S. P. 1995. Photoreactions of the photointermediates of bacteriorhodopsin. *Isr. J. Chem.* 35:415–428.

Balashov, S. P., and F. F. Litvin. 1981. Photochemical conversions of bacteriorhodopsin. *Biophysics.* 25:566–581.

Bashford, D., and K. Gerwert, 1992. Electrostatic calculations of the pKa values of ionizable groups in bacteriorhodopsin. *J. Mol. Biol.* 224: 473–486.

Bousché, O., M. Braiman, Y.-W. He, T. Marti, H. G. Khorana, and K. J. Rothschild. 1991. Vibrational spectroscopy of bacteriorhodopsin mutants. *J. Biol. Chem.* 266:11063–11067.

Braiman, M. S., T. Mogi, T. Marti, L. J. Stern, H. G. Khorana, and K. J. Rothschild. 1988a. Vibrational spectroscopy of Bacteriorhodopsin mutants: light-driven proton transport involves protonation changes of aspartic acid residues 85, 96 and 212. *Biochemistry.* 27:8516–8520.

Braiman, M. S., T. Mogi, L. J. Stern, N. R. Hackett, B. H. Chao, H. G. Khorana, and K. J. Rothschild. 1988b. Vibrational spectroscopy of Bacteriorhodopsin mutants. I. Tyrosine-185 protonates and deprotonates during the photocycle. *Proteins Struct. Funct. Genet.* 3:219–229.

Brown, L. S., J. Sasaki, H. Kandori, A. Maeda, R. Needleman, and J. K. Lanyi. 1995. Glutamic acid 204 is the terminal proton release group at the extracellular surface of bacteriorhodopsin. *J. Biol. Chem.* 270: 27122–27126.

De Grip, W. J., and H. Watts (Editors). 1995 Retinal proteins, Special issue of *Biophys. Chem.* 56:1–2.

Druckmann, S., N. Friedmann, J. K. Lanyi, R. Needleman, M. Ottolenghi, and M. Shewes. 1992. The back photoreaction of the M intermediate in the photocycle of bacteriorhodopsin: mechanism and evidence for two M species. *Photochem. Photobiol.* 56:1041–1047.

Druckmann, S., M. P. Heyn, J. K. Lanyi, M. Ottolenghi, and L. Zimányi. 1993. Thermal equilibrium between the M and the N intermediates in the photocycle of bacteriorhodopsin. *Biophys. J.* 65:1231–1234.

Eisfeld, W., C. Pusch, R. Diller, R. Lohrmann, and M Stockburger. 1993. Resonance Raman and optical transient studies on the light-induced proton pump of bacteriorhodopsin reveal parallel photocycles. *Biochemistry.* 32:7196–7215.

Engelhard, M., K. Gerwert, B. Hess, W. Kreutz, and F. Siebert. 1985. Light-driven protonation of internal aspartic acids of bacteriorhodopsin: an investigation by static and time-resolved infrared difference spectroscopy using [4-^{13}C]aspartic acid labeled purple membrane. *Biochemistry.* 24:400–407.

Fahmy, K., O. Weidlich, M. Engelhard, J. Tittor, D. Oesterheld, and F. Siebert. 1992. Identification of the proton acceptor of Schiff base deprotonation in bacteriorhodopsin: a Fourier transform infrared study on the mutant $Asp^{85}\rightarrow Glu$ in its natural lipid environment. *Photochem. Photobiol.* 56:1073–1083.

Fodor, S. P. A., J. B. Ames, R. Gebhard, E. M. M. van den Berg, W. Stoeckenius, J. Lugtenburg, and R. A. Mathies. 1988. Chromophore structure in bacteriorhodopsin's N intermediate: implications for the proton-pumping mechanism. *Biochemistry.* 27:7097–7101.

Gerwert, K., B. Hess, and M. Engelhard. 1990b. Proline residues undergo structural changes during proton pumping in bacteriorhodopsin. *FEBS Lett.* 261:449–459.

Gerwert, K., B. Hess, J. Soppa, and D. Oesterhelt. 1989. The role of Asp^{96} in the proton pump mechanism of bacteriorhodopsin. *Proc. Natl. Acad. Sci. USA.* 86:4943–4947.

Gerwert, K., and F. Siebert. 1986. Evidence for light-induced 13-cis,14-s-cis isomerization in bacteriorhodopsin obtained by FTIR difference spectroscopy using isotopically labelled retinals. *EMBO J.* 5:805–811.

Gerwert, K., G. Souvignier, and B. Hess. 1990a. Simultaneous monitoring of light-induced changes in protein side-group protonation, chromophore isomerization, and backbone motion of bacteriorhodopsin by time-resolved Fourier-transform infrared spectroscopy. *Proc. Natl. Acad. Sci. USA.* 87:9774–9778.

Grigorieff, N., T. A. Ceska, K. H. Downing, J. M. Baldwin, and R. Henderson. 1996. Electron-crystallographic refinement of the structure of bacteriorhodopsin. *J. Biol. Chem.* 259:393–421.

Hage, W., M. Kim, H. Frei, and R. A. Mathies. 1996. Protein dynamics in the bacteriorhodopsin photocycle: a nanosecond step-scan FTIR investigation of the KL to L transition. *J. Phys. Chem.* 100:16026–16033.

Herzfeld, J., S. K. Das Gupta, M. R. Farrar, G. S. Harbison, A. E. McDermott, S. L. Pelletier, D. P. Raleigh, S. O. Smith, C. Winkel, J. Lugtenburg, and R. G. Griffin. 1990. Solid-state ^{13}C NMR study of tyrosine protonation in dark-adapted bacteriorhodopsin. *Biochemistry.* 29:5567–5574.

Hessling, B., G. Souvignier, and K. Gerwert. 1993. A model-independent approach to assigning bacteriorhodopsin's intramolecular reactions to photocycle intermediates. *Biophys. J.* 64:1929–1941.

Hurley, J. B., B. Becher, and T. Ebrey. 1978. More evidence that light isomerises the chromophore of purple membrane protein. *Nature.* 272: 87–88.

Kalisky, O., U. Lachish, and M. Ottolenghi. 1977. Time resolution of a back photoreaction in bacteriorhodopsin. *Photochem. Photobiol.* 28: 261–263.

Koch, M. H. J., N. A. Dencher, D. Oesterhelt, H.-J. Plöhn, G. Rapp, and G. Büldt. 1991. Time-resolved X-ray diffraction study of structural changes associated with the photocycle of bacteriorhodopsin. *EMBO J.* 10: 521–526.

Kochendoerfer, G. G., Z. Wang, D. D. Oprian, and R. A. Mathies. 1997. Resonance Raman examination of the wavelength regulation mechanism in human visual pigments. *Biochemistry.* 36:6577–6587.

Lanyi, J. K., and G. Váró. 1995. The photocycles of bacteriorhodopsin. *Isr. J. Chem.* 35:365–385.

le Coutre, J., and K. Gerwert. 1996. Kinetic isotope effects reveal an ice-like and a liquid-phase-type intramolecular proton transfer in bacteriorhodopsin. *FEBS Lett.* 398:333–336.

le Coutre, J., J. Tittor, D. Oesterhelt, and K. Gerwert. 1995. Experimental evidence for hydrogen-bonded network proton transfer in bacteriorhodopsin shown by FTIR spectroscopy using azide as catalyst. *Proc. Natl. Acad. Sci. USA.* 92:4962–4966.

Liu, X.-M., S. Sonar, C.-P. Lee, M. Coleman, U. L. Rajbhandary, and K. J. Rothschild. 1995. Site-directed isotope labeling and FTIR spectroscopy: assignment of tyrosine bands in the $bR\rightarrow M$ difference spectrum of bacteriorhodopsin. *Biophys. Chem.* 56:63–70.

Lozier, R. H., R. A. Bogomolni, and W. Stoeckenius. 1975. Bacteriorhodopsin: a light-driven proton pump in *Halobacterium halobium. Biophys. J.* 15:955–962.

Malinowski, E. R. 1980. Factor Analysis in Chemistry. John Wiley and Sons, New York.

McDermott, A. E., L. K. Thompson, C. Winkel, M. R. Farrar, S. Pelletier, J. Lugtenburg, J. Herzfeld, and R. G. Griffin. 1991. Mechanism of proton pumping in bacteriorhodopsin by solid-state NMR: the protonation state of tyrosine in the light-adapted and M states. *Biochemistry.* 30:8366–8371.

Oesterhelt, D., and W. Stoeckenius. 1971. Rhodopsin-like protein from the purple membrane of *Halobacterium halobium. Nature New Biol.* 233: 149–152.

Oesterhelt, D., and W. Stoeckenius. 1974. Isolation of the cell membrane of *Halobacterium halobium* and its fractionation into red and purple membrane. *Methods Enzymol.* 31:667–678.

Ormos, P. 1991. Infrared spectroscopic demonstration of a conformational change in bacteriorhodopsin involved in proton pumping. *Proc. Natl. Acad. Sci. USA.* 88:473–477.

Ormos, P., K. Chu, and J. Mourant. 1992. Infrared study of the L, M, and N Intermediates of bacteriorhodopsin using the photoreaction of M. *Biochemistry.* 31:693–6937.

Perkins, G. A., E. Liu, F. Burkard, E. A. Berry, and R. M. Glaeser. 1992. Characterization of the conformational change in the M_1 and M_2 substates of bacteriorhodopsin by the combined use of visible and infrared spectroscopy. *J. Struct. Biol.* 1029:142–151.

Pfefferlé, J. M., A. Maeda, J. Sasaki, and T. Yozikawa. 1991. Fourier transform infrared study of the N intermediate of bacteriorhodopsin. *Biochemistry.* 30:6548–6556.

Plunkett, S. E., J. L. Chao, T. J. Tague, and R. A. Palmer. 1995. Time-resolved step-scan FT-IR spectroscopy of the photodynamics of carbonmonoxymyoglobin. *Appl. Spectrosc.* 49:702–708.

Rammelsberg, R., B. Hessling, H. Chorongiewski, and K. Gerwert. 1997. Molecular reaction mechanisms of protein monitored by nanosecond step-scan FT-IR difference spectroscopy. *Appl. Spectrosc.* 51:558–562.

Rüdiger, R., U. Haupts, K. Gerwert, and D. Oesterhelt. 1995. Chemical reconstitution of a chloride pump inactivated by a single point mutation. *EMBO J.* 14:1599–1606.

Sampogna, R. V., and B. Honig. 1996. Electrostatic coupling between retinal isomerization and the ionization state of Glu-204—a general mechanism for proton release in bacteriorhodopsin. *Biophys. J.* 71: 1165–1171.

Sasaki, J., Y. Shichida, J. K. Lanyi, and A. Maeda. 1992. Protein changes associated with reprotonation of the Schiff base in the photocycle of $Asp^{96}\rightarrow Asn$ bacteriorhodopsin. The M_n intermediate with unprotonated Schiff base but an N-like protein structure. *J. Biol. Chem.* 267: 20782–20786.

Scharnagl, C., J. Hettenkofer, and S. F. Fischer. 1995. Electrostatic and conformational effects on the proton translocation steps in bacteriorhodopsin: analysis of multiple M structures. *J. Phys. Chem.* 99:7787–7800.

Schulten, K., Z. Schulten, and P. Tavan. 1984. An isomerization model for the pump cycle of bacteriorhodopsin. *In* Information and Energy Transduction in Biological Membranes. A. Bolis, H. Helmreich, and H. Passow, editors. Alan R. Liss, New York. 113–131.

Schulten, K., and P. Tavan. 1978. A mechanism for the light-driven proton pump of *Halobacterium halobium. Nature.* 272:85–86.

Smith, S. O., M. S. Braiman, A. B. Myers, J. A. Pardoen, J. M. L. Courtin, C. Winkel, J. Lugtenburg, and R. A. Mathies. 1987. Vibrational analysis of the all-*trans*-retinal chromophore in light-adapted bacteriorhodosin. *J. Am. Chem. Soc.* 109:3108–3125.

Smith, S. O., J. A. Pardoen, P. P. J. Mulder, B. Curry, J. Lugtenburg, and R. A. Mathies. 1983. Chromophore structure in bacteriorhodopsin's O640 photointermediate. *Biochemistry.* 22:6141–6148.

Souvignier, G., and K. Gerwert. 1992. Proton uptake mechanism of bacteriorhodopsin as determined by time-resolved stroboscopic-FTIR-spectroscopy. *Biophys. J.* 63:1393–1405.

Subramaniam, S., M. Gerstein, D. Oesterhelt, and R. Henderson. 1993. Electron diffraction analysis of structural changes in the photocycle of bacteriorhodopsin. *EMBO J.* 12:1–8.

Takei, H., Y. Gat, M. Sheves, and A. Lewis. 1992. Low temperature FTIR study of the Schiff base reprotonation during the M to bR back-photoreaction. *Biophys. J.* 63:1643–1653.

Uhmann, W., A. Becker, C. Taran, and F. Siebert. 1991. Time-resolved FT-IR absorption spectroscopy using a step-scan interferometer. *Appl. Spectrosc.* 45:390–397.

Váró, G., and J. K. Lanyi. 1991a. Kinetic and spectroscopic evidence for an irreversible step between deprotonation and reprotonation of the Schiff base in the bacteriorhodopsin photocycle. *Biochemistry.* 30: 5008–5015.

Váró, G., and J. K. Lanyi. 1991b. Thermodynamics and energy coupling in the bacteriorhodopsin photocycle. *Biochemistry.* 30:5016–5022.

Weidlich, O., and F. Siebert. 1993. Time-resolved step-scan FT-IR investigations on the transition from KL to L in the bacteriorhodopsin photocycle: identification of chromophore twists by assigning hydrogen out-of-plane (HOOP) bending vibrations. *Appl. Spectrosc.* 47: 1394–1400.

Xie, A. H., J. F. Nagle, and R. H. Lozier. 1987. Flash spectroscopy of purple membrane. *Biophys. J.* 51:627–635.

Xu, D., M. Sheves, and K. Schulten. 1995. Molecular dynamics study of the M412 intermediate of bacteriorhodopsin. *Biophys. J.* 69:2745–2760.

Zimányi, L., Y. Cao, M. Chang, B. Ni, R. Needleman, and J. K. Lanyi. 1992. The two consecutive M substates in the photocycle of bacteriorhodopsin are affected specifically by the D85N and D96N residue replacements. *Photochem. Photobiol.* 56:1049–1055.